Nanotitania catalyzes the chemoselective hydration and alkoxylation of epoxides

Judit Oliver–Meseguer [a], Jordi Ballesteros–Soberanas [a], María Tejeda–Serrano [a],
Aarón Martínez–Castelló [b], Antonio Leyva–Pérez [a,*]

[a] *Instituto de Tecnología Química (UPV–CSIC), Universidad Politècnica de València–Consejo Superior de Investigaciones Científicas, Avda. de los Naranjos s/n, 46022 Valencia, Spain*
[b] *Zschimmer & Schwarz Spain, CTRA. CV–20, KM. 3.200. APDO. 118, 12540 Villareal, Spain*

ARTICLE INFO

ABSTRACT

Glycols and ethoxy– and propoxy–alcohols are fundamental chemicals in industry, with annual productions of millions of tons, still manufactured in many cases with corrosive and unrecoverable catalysts such as KOH, amines and $BF_3 \bullet OEt_2$. Here we show that commercially available, inexpensive, non–toxic, solid and recyclable nanotitania catalyzes the hydration and alkoxylation of epoxides, with water and primary and secondary alcohols but not with phenols, carboxylic acids and tertiary alcohols. In this way, the chemoselective synthesis of different glycols and 1,4–dioxanones, and the implementation of nanotitania for the production in–flow of glycols and alkoxylated alcohols, has been achieved. Mechanistic studies support the key role of vacancies in the nano–oxide catalyst.

1. Introduction

The opening of epoxides by hydroxyl groups, i.e. hydration and alkoxylation reactions, is the highest industrial catalyzed organic reactions in volume per year [1]. The hydration reaction can be carried out under uncatalyzed conditions at high water dilution and reaction temperature, however, the process is low selective and very energy intensive (after distillations) to monoethyl glycol (MEG), thus, in practice, is performed under catalyzed conditions. Indeed, the acid–catalyzed OMEGA ("Only MEG Advantage") process, developed by Shell, makes use of acid catalysts to convert ethylene epoxide to ethylene carbonate with CO_2, and then to hydrolyze them back to MEG [2,3]. Following this, the alkoxylation reaction, also named ethoxylation and propoxylation reaction of ethylene and propylene epoxide, respectively, is also catalyzed, as shown in Fig. 1.

It can be seen above that either strong bases or acids catalyze the epoxide opening reaction, since acids activate the epoxide and bases activate the alcohols. The base–catalyzed approach is industrially more common since the uncontrolled self–opening and polymerization of the epoxide (i.e. by traces of water) occurs in high extent under strong acid conditions. In any case, the industrial reaction conditions require a strict control of the process, including slow addition of the epoxide and careful temperature and pressure control, in order to circumvent the formation of polyalkoxyglycols and thermal runaways associated to the use of such strong bases or acids. It was envisioned here that a much milder catalytic system could be achieved by the concomitant use of a weak base and a weak acid, together, to better control the reaction pathways, enhancing the target reactions and minimizing undesired by–reactions, as also shown in Fig. 1. Of course, acids and bases are incompatible in solution, however, in our approach here, both functions are located in a solid as a soft acid–base pair, where both the epoxide (electrophile) and water or alcohol (nucleophiles) are activated at the same time for the desired coupling [4].

The base and acid functions of the new catalyst must fulfill at least two fundamental conditions: avoid quenching each other during reaction and being located at an atomic distance from each other to activate the coupling partners. For that, we decided to explore commercially––available nanosized solids, able to perform this bifunctional catalytic function. Nanosizing completely changes the catalytic properties of macroscopic solids [5–8], providing high surface areas with coordinatively unsaturated metal atoms and neighboring oxygen vacancies [9,10], which can be considered as frustrated Lewis acid–base sites [11]. These nanosolids have already been successfully used as catalysts for alcohol activation and epoxide activation, separately, but not for the
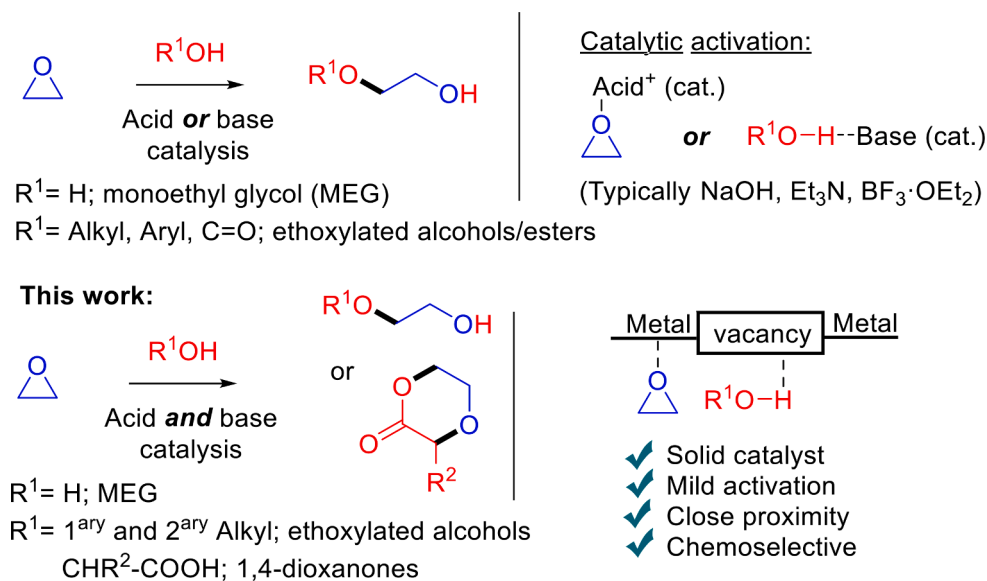
Fig. 1. Industrial synthesis of glycols and ethoxylated alcohols and esters catalyzed by strong bases and acids (top) and the approach in this work, with bifunctional nano–oxides (bottom).

concomitant activation of both functionalities in the hydration and alkoxylation reaction [12,13]. In particular, the hydration of epoxides has been performed with silica–based catalysts [14–16], solid strong bases [17], zeolites [18,19], and porous organic frameworks [20], among others [21–26]. However, it is difficult to find in the recent open literature studies related to the application of nanostructured solid catalytic materials for the alkoxylation reaction [21,27,28], which may explain why it is still industrially performed with old catalysts such as KOH, amines or strong Lewis acids such as $BF_3 \bullet OEt_2$. Thus, it seemed reasonable to test solid nano–oxides as catalysts for the epoxide opening with water and alcohols.

2. Materials and methods

2.1. General

Reagents were obtained from commercial sources (Merck–Aldrich) and used without further purification otherwise indicated. Nanotitania was purchased from NanoScale Corporation and nanosized cerium oxide was purchased from Rhodia Co. The other nanoceria materials were prepared according to previously published methods [29,30]. Dried and deaerated THF solvent, when required, was obtained after treatment with purification resins, having less than 50 ppm of water. All the products obtained were characterized by GC and GC–MS if the molecular weight allowed these techniques (mainly for glycolic acid derivatives), and ^{1}H–, ^{13}C–NMR and DEPT. When available, the characterization given in the literature was used for comparison. Gas chromatographic analyses were performed in an instrument equipped with a 25 m capillary column of 1% phenylmethylsilicone. GC–MS analyses were performed on a spectrometer equipped with the same column as the GC and operated under the same conditions. NMR were recorded in a 300 MHz instrument using the appropriate solvent containing TMS as an internal standard. Solid IR spectra were recorded on a spectrophotometer by previous mixture of the solid with dried KBr. Electron microscopy studies were performed on a microscope operated at 100–200 kV after impregnating a dispersion of the solid sample on a Cu grid and leaving to evaporate for, at least, 4 h. Specific rotations were measured in a polarimeter using a sodium D light source and a 10 cm path length cuvette, under the indicated temperature, after dissolving the corresponding compounds in 1 ml of MeOH or EtOH. Field emission scanning electron microscopy images (FESEM) were taken with a Zeiss

Ultra 55 instrument. Transmission electron microscopy (TEM) measurements were carried out in a JEOL instrument. To calculate the surface area, the instrument used was Micromeritics ASAP2020, using the method Brunauer-Emmett-Teller (BET) using the adsorption isotherms.

2.2. Reaction procedure for alkoxylations with soluble catalysts

Ethylene oxide in THF (0.9 ml, 3 mmol, 3.3 M) and the corresponding amount of catalyst (0.1 mol%, 0.00025 mmol, see Table S1) were placed in a double–walled 6 mL vial, equipped with a magnetic stirrer. The reactor was closed with a screw cap connected to a manometer. The reactor was purged three times with N_2 and finally charged with 3 bars of N_2. The reaction mixture was placed in a pre–heated oil bath at 70 °C and magnetically stirred over 16 h. At the end of the reaction, the mixture was cooled, concentrated and analyzed by ^{1}H–NMR.

2.3. Reaction procedure for alkoxylations with solid catalyst

The corresponding nucleophile (water or alcohol, typically 0.5 mmol), 1.8 ml of ethylene oxide in THF (6 mmol, 3.3 M) and 65 mg of solid catalyst (25 wt%) were placed in a double–walled 6 mL vial, equipped with a magnetic stirrer. The reactor was closed with a screw cap connected to a manometer. The reactor was purged three times with N_2 and finally charged with 3 bars of N_2. The reaction mixture was placed in a pre–heated oil bath at 120 °C and magnetically stirred over 16 h. At the end of the reaction, the mixture was cooled, filtered, concentrated and analyzed by ^{1}H–NMR and GC–MS.

2.4. Reaction procedure for ethylene and propylene epoxide co–oligomerization

Different amounts of ethylene and propylene oxide (6 mmol) and 65 mg of TiO_2 (25 wt%) were placed in a double–walled 6 mL vial, equipped with a magnetic stirrer. The reactor was closed with a screw cap connected to a manometer. The reactor was purged three times with N_2 and finally charged with 3 bars of N_2. The reaction mixture was placed in a pre–heated oil bath at 150 °C and magnetically stirred over 2–24 h. At the end of the reaction, the mixture was cooled, filtered, concentrated and analyzed by ^{1}H–NMR.

Table 1

Results for the hydration/oligomerization of ethylene epoxide 1a or propylene epoxide 1b with different catalysts. 1a was added as 3.3 M solution in THF. Batch reaction.

Entry	Catalyst (wt%)	Epoxide	H_2O (equiv.)	T ($^\circ$C)	Isolated yield (%)[b]	Product distribution			
						2	3	4	5
1	None	**1a**	–	70	0	–			
2[a]	$BF_3 \bullet OEt_2$ (0.2)				>99				
3[a]	$FeCl_3$ (0.2)				0				
4[a]	$ZnBr_2$ (0.2)				<1				
5	Et_3N (2)				0				
6	Bu_3N (2)				<1				
7	nano–MgO (25)				5				
8	nano–ZrO_2 (25)				7				
9	nanoCeO$_2$ (25)				17				
10	nano–TiO_2 (25)				37				
11	TiO_2				2				
12	None			120	9				
13	nano–TiO_2 (25)				42	–	15	51	34
14		**1b**			14	–	44	44	12
15[c]	nano–TiO_2 (50)	**1a**		150	46	–			
16		**1a + 1b** (1:3)			54				
17		**1a + 1b** (1:1)			37				
18	nano–TiO_2 (25)	**1a**	1	120	81	32	57	6	5
19		**1b**			33	43	54	3	–
20		**1a**	3		98	64	31	3	2
21		**1b**			61	83	16	1	–
22		**1a**	5		>99	68	27	4	1
23		**1b**			65	85	14	<1	–

[a] ca. 0.1 mol%, see Table S1.
[b] Weight of recovered products after filtration and washings of the solid with dichloromethane and methanol, combination with the Soxhlet extracts of the solid, and vacuum concentration. [c] See kinetics below.

2.5. Typical reaction procedure for reusing nanotitania in batch

Water (5.5 eq), propylene oxide (6.6 mmol) and 130 mg of nano–titania (35 wt%) were placed in a double–walled 6 mL vial, equipped with a magnetic stirrer. The reactor was closed with a screw cap connected to a manometer. The reactor was purged three times with N_2 and finally charged with 3 bars of N_2. The reaction mixture was placed in a pre–heated oil bath at 120 $^\circ$C and magnetically stirred over 20 h. At the end of the reaction, the mixture was cooled, washed with methanol and hexane the catalyst, filtered, concentrated, and weighted to analyze by GC–MS. The catalyst was dried at 120 $^\circ$C during 2 h before using again.

2.6. Typical reaction procedure for kinetics with different solid catalysts in batch

Water (5.5 eq), propylene oxide (6.6 mmol) and 95 mg of nanotitania or nanoceria (doped or not, 25 wt%) were placed in a double–walled 6 mL vial, equipped with a magnetic stirrer. The reactor was closed with a screw cap connected to a manometer. The reactor was purged three times with N_2 and finally charged with 3 bars of N_2. The reaction mixture was placed in a pre–heated oil bath at 120 $^\circ$C and magnetically stirred taking samples at the indicated times to analyze by GC–MS.

2.7. Typical reaction procedure in flow for the ethoxylation with nanotitania

A lab–scale packed bed reactor was used in the continuous flow re-actions (see Figure S3). The reactor was connected to a heat source and was insulated to ensure the temperature across the reactor remained uniform. A small wadding of glass cotton was placed at the bottom of the reactor (outlet) and tungsten carbide (packing material) was packed ¾ of the way up the reactor. 0.5 g of pelletized (0.2–0.4 mm) nano–TiO2 was then inserted into the reactor and tungsten carbide was used to pack the rest of the reactor to the top. The reactor was then heated at 120 $^\circ$C. There was an inlet at the top of the reactor for introducing the reaction mixture (15 ml ethylene oxide 3.3 M in THF). The inlet was connected to a syringe and the mixture was pumped into the reactor at 0.02 ml•min^{-1}.

2.8. Procedure to ethoxylate 12–HSA **8a** without catalyst

150 mg of 12–HSA **8a** (1 eq, 0.5 mmol) and 0.5 ml of ethylene oxide in THF (12 eq, 6 mmol, 3 M) were placed in a 6 mL vial, equipped with a magnetic stirrer. The reactor was closed with a screw cap connected to a manometer. The reactor was purged three times with N_2 and finally charged with 3 bars of N_2. The reaction mixture was placed in a pre--heated oil bath at 120 $^\circ$C and magnetically stirred overnight (16 h). At the end of the reaction, the mixture was cooled, quenched with $KHCO_3$ saturated in MeOH, filtered, concentrated and analyzed by ^{1}H–, ^{13}C–NMR, and DEPT.

2.9. Procedure to ethoxylate 12–HSA **8a** with nano–TiO_2

150 mg of 12–HSA **8a** (1 eq, 0.5 mmol), 0.5 ml ethylene oxide in THF (12 eq, 6 mmol, 3 M) and 65 mg of nano–TiO_2 solid catalyst (40 wt%) were placed in a 6 mL vial, equipped with a magnetic stirrer. The reactor was closed with a screw cap connected to a manometer. The reactor was purged three times with N_2 and finally charged with 3 bars of N_2. The reaction mixture was placed in a pre–heated oil bath at 120 $^\circ$C and magnetically stirred overnight (16 h). At the end of the reaction, the mixture was cooled, quenched with $KHCO_3$ saturated in MeOH, filtered, concentrated and analyzed by ^{1}H–NMR. The product **9a** was obtained as a solid at room temperature (20 $^\circ$C) but became liquid at 40 $^\circ$C.

2.10. Typical reaction procedure in flow for the propoxylation with nanotitania

Reactions were performed in a continuous flow reactor, where the catalyst was placed in between glass wool inside a 0.5 in. diameter steel tube (see Figure S3). The reactor was connected to a heat source and was insulated to ensure the temperature across the reactor remained uni-form. A small wadding of glass wool was placed at the bottom of the reactor (outlet). 0.5 g to 2 g of nano–TiO_2 were then loaded, and another small glass wool wadding was placed on top, to secure the packed bed. The catalyst powder was purged at room temperature with N_2 for 15 min and heated to reaction temperature in the same inert gas, prior to
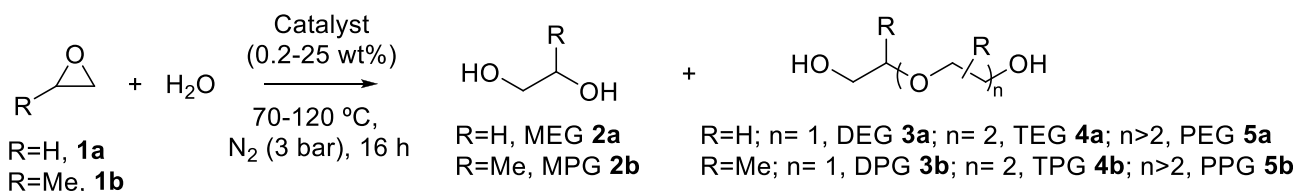
introducing the reactants in the system. Reaction were performed at temperatures ranging from 125 to 200 °C. N_2 was used as the carrier; it was bubbled through the liquid phase reactant mixture (15:85, propylene oxide: methanol) inside a temperature–controlled bath set at 15 °C. Pressure was always kept at atmospheric levels, and the flow rate was set at 5 sccm. In order to analyze the reaction products, the reaction mixture was immediately cooled down upon exiting the reactor by bubbling the outlet flow through a short, thin capillary into a *n*–heptanol bath at −20 °C.
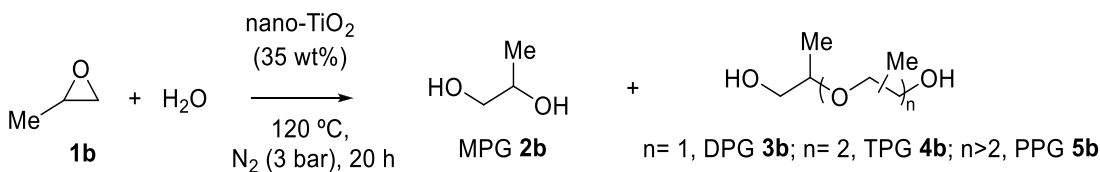
3. Results and discussion

3.1. Synthesis of ethylene glycols catalyzed by nano–TiO₂

3.1.1. In batch

Table 1 shows the catalytic results for the ring opening of ethylene epoxide **1a** or propylene epoxide **1b** with or without water, to give glycols **2–5** as products. For the sake of comparison, the reactions were performed in all cases with the reagents and the catalyst placed at once in an autoclave, equipped with a magnetic bar and filled up to 3 bar of inert atmosphere, without reagent or catalyst dosification. It is worth mentioning that these reaction conditions may differ from those in industry, where a very careful dosing of reagents/catalyst is carried out, but it allows for a fair comparison between catalysts.

chromatography coupled to mass spectrometry (GC–MS) measurements. Fig. 2 shows the kinetics of the reaction at 150 °C (entry 15 in Table 1), where it can be seen that **1a** rapidly evolves to the corresponding glycols in the first 2 h of reaction, up to 18% yield, and then smoothly reacts during the following 15 h to achieve a final 46% yield. It is worthy to saying here that a ca. 25 nm particle size for nanotitania gets exposed <10% of the total atoms of the oxide, and only a fraction of these atoms are vacancies, thus <2.5 wt% of atoms are effectively doing the catalysis.

This kinetic profile is in good agreement with a good reactivity of the smaller alcohols derived from **1a**, thus circumventing uncontrolled polymerizations. In accordance with this hypothesis, propylene oxide **1b** should be less reactive than **1a** over the nano–TiO₂ catalyst, due to the higher steric hindrance imparted by the methyl group around the epoxide, which indeed occurs (entry 14 in Table 1). However, following the same rationale, it could occur that **1a** helps to activate **1b** (Figure S2), thus improving the reactivity of **1b** and forming co–glycols of interest in industry [34]. The results show that, indeed, **1b** reacts faster in the presence of **1a**, to give a higher glycol yield than when **1b** is treated alone (entries 15–16). This methodology, if the nano–TiO₂ catalyst is not removed, may also enable the formation of pegylated nano–TiO₂ with potential biological applications [35–37].
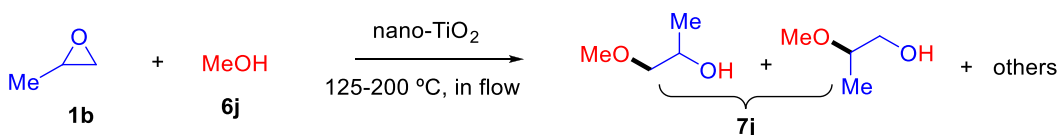
At this point, and in order to obtain monoglycols **2a–b**, water was added as a reagent to the reaction. For ethylene epoxide **1a**, the addition

Catalyst (0.2-25 wt%)

70-120 ºC, N_2 (3 bar), 16 h

R=H, **1a**
R=Me, **1b**

R=H, MEG **2a**
R=Me, MPG **2b**

R=H; n= 1, DEG **3a**; n= 2, TEG **4a**; n>2, PEG **5a**
R=Me; n= 1, DPG **3b**; n= 2, TPG **4b**; n>2, PPG **5b**

The results show that, if water is not added and conventional Lewis acid salts are used as catalysts at 70 °C (entries 1–4), the reaction only proceeds with the very strong acid BF₃•OEt₂ (entry 2), to give an uncontrolled polymeric mixture according to proton nuclear magnetic resonance (^{1}H–NMR) and isolated weight [31]. Tertiary amines are also ineffective under our reaction conditions (entries 5–6). However, nano–oxides such as nano–MgO, nano–ZrO₂, nano–CeO₂ and, particularly, nano–TiO₂ (entries 7–10) give reasonable amounts of isolated glycols, after exhaustive washing of the solid catalyst (see Table S2 for physicochemical properties of the nanomaterials and Figure S1 for characterization, including X-ray diffraction (XRD) measurements and field emission scanning electronic microscopy (FESEM) photographs)

of just 3–5 equivalents of water are enough to achieve nearly quantitative conversions and a ~65% yield of MEG **2a** (see entries 15, 17 and 19). Propylene epoxide **1b**, despite being less reactive, converts in a reasonable ~60% with a good 85% selectivity towards monopropylene glycol (MPG) **3b**. These results for the monoglycols **2a–b** are remarkable considering the low amount of water added, since the industrial production of **2a** uses 20 equivalents of water and only particular catalysts are able to decrease that amount down to 8 equivalents [21]. Here, nano–TiO₂ requires just 3 equivalents of water, which, compared to other systems, translates into the handling of less than half the volume of reaction, thus doubling the throughput of the reaction. Besides, Fig. 3 shows that the catalyst could be reused up to 6 times mantaining the conversion and selectivity of the reaction.

nano-TiO₂ (35 wt%)

120 ºC, N_2 (3 bar), 20 h

1b

MPG **2b**

n= 1, DPG **3b**; n= 2, TPG **4b**; n>2, PPG **5b**

[32,33]. Notice that conventional commercial anatase TiO₂, with the same polymorphic form that nano–TiO₂, barely catalyzes the reaction (entry 11).

In order to improve the reaction rate, the temperature was increased to 120 °C. At this reaction temperature, the non–catalyzed reaction of ethylene oxide **1a** yielded a 9% of glycols (entry 12) and, in clear contrast, nano–TiO₂ gave a 42% of glycols **3a–5a**, with triethylenglycol (TEG) **4a** as the main component of the mixture and without a trace of monoethylenglycol (MEG) **2a** (entry 13), according to gas

3.1.2. In–flow liquid–phase ethoxylation

With the above results in hand, and given that nano–TiO₂ is a robust and pelletizable solid, the synthesis of glycols in flow, from ethylene oxide **1a** dissolved in THF, was attempted. The reactor consists in a lab–scale tubular, packed bed reactor connected to a heat source, filled with tungsten carbide (packing material) ¾ of the way up the reactor, 0.5 g of nano–TiO₂, and more tungsten carbide to fill the remaining

reactor length (Figure S3). An inlet connected to a syringe is employed to feed the solution of **1a** in THF at the top of the reactor, and nano–TiO$_2$ was pelletized to 0.2–0.4 mm size. With this set–up in hand, the calculation of the starting reaction conditions was made on the basis of the corresponding results in batch. For instance, the kinetic profile in Fig. 2 above indicates that a spatial velocity of 0.02 ml•min^{-1} for **1a** should be enough to reproduce the batch results. Indeed, a 40% yield of **1a** to the corresponding glycols **2a–5a** was consistently obtained during 3 h on stream. These results open the way for the in–flow production of glycols under realistic gas–phase conditions (see below).

single–pass propylene oxide conversion increased with temperature, but selectivity towards the desired coupling products **7j** decreases sharply above 150 °C (Figure S9). With fresh catalyst, the reaction was performed again for 21 h at 150 °C, with a lower WHSV of 0.03 h^{-1}, to achieve full propylene oxide conversion. The reactor outlet was monitored for the full length of the experiment, and the steady state was reached after approximately 5 h, when the flow rate of products and reactants remained stable at 0.79 ± 0.10 mg/min, and matched that of the inlet, 0.80 mg/min (Figure S10).

3.2. Alkoxylation of alcohols catalyzed by nano–TiO$_2$

3.2.1. In batch: synthesis of 1,2–dioxanones

Fig. 4 shows the alkoxylation of **1a** or **1b** with the different alcohols **6a–h** catalyzed by nano–TiO$_2$ at 120 °C after 16 h, to give products **7a–h**, also including industrially–relevant examples. For instance, lauryl alcohol **6a** is readily ethoxylated to give product **7a**, with 5 ethoxy units incorporated in average, according to ^{1}H–NMR (Figure S4). Other alcohols incorporating additional functionalities such as alkyne (**7c**), alkene (**7d** and 7 h), cyano (**7e**), ketone (**7f**) and tertiary alcohol (7 g) were also reactive. Fourier–transformed infrared analysis (FT–IR) of the fresh and used nano–TiO$_2$ catalyst shows that just marginal amounts of organic compounds remain on the solid surface after reaction (Figure S5).

Ethoxylated castor oil is a high–volume industrial chemical, annually produced in multi–ton amounts [38]. Thus, we proceeded to ethoxylate 12–hydroxysteraric acid (12–HSA) **8a**, a surrogate of castor oil (Figure S6), under the nano–TiO$_2$ catalyzed conditions. The corresponding product **9a**, exclusively ethoxylated in the alcohol but not in the carboxylic group, with 4 ethoxy units in average, was obtained (Figure S7). This chemoselective reaction must be remarked, since generally carboxylic groups are readily ethoxylated even in the presence of alcohol but, in contrast, nano–TiO$_2$ prevented carboxylic ethoxylations while promoting alcohol ethoxylations [39]. We confirmed this reactivity by performing the ethoxylation of **8a** without catalyst, and observing the preferential ethoxylation of the carboxylic group (Figure S8). With these results in hand, we tested hydroxyacid compounds **8b–f** as substrates for the alkoxylation reaction, as shown in Fig. 5. In particular, it was envisioned that the chemoselective alcohol ethoxylation of 2–hydroxyacids would trigger a spontaneous intramolecular esterification between the newly incorporated ethoxy group and the untouched free carboxylic acid [40]. This reactivity supposes a new retrosynthetic strategy for 1,4–dioxenones, a functionality present in natural products [41] which do not have, to our knowledge, any general synthetic approach beyond oxidations of dioxanes [42–49].

Products **9b–i** where obtained in good yields, including a variety of 1,4–dioxenones. The latter were obtained with tolerance to other functional groups and keeping the optical rotation of the chiral hydroxyacid carbon atom (products **9h–i**). These results open a new way towards the synthesis of 1,4–dioxenones, with the additional advantage of using a simple solid catalyst.

3.2.2. In–flow gas–phase propoxylation

Fig. 6 shows that the nano–TiO$_2$ catalyst was active in flow conditions for the gas phase methanol propoxylation to give products **7j**. The reaction was performed at 125, 150, 175 and 200 °C, with a WHSV (weight hourly spatial velocity) of 0.12 h^{-1}. Propylene oxide **1b** was the limiting reactant, and methanol **6j** was fed in excess, 3 to 1. The

At the steady state, the propylene oxide conversion oscillated between 95 and 98%, and the selectivity towards alkoxylation products **7j**, self–opening propylene oxide products **3b-5b** and other products were 62%, 36% and 2%, respectively. Remarkably, the reaction almost exclusively yielded the regioselective mixture 1–methoxypropan–2–ol and 2–methoxypropan–1–ol **7j**, roughly 1:1 at the steady state, with only traces of **3b-5b**. Notice that the hydrated product **2b** was not observed since the in–flow reaction conditions allows a complete dryness of the system. A larger residence time inside the packed bed time resulted in a complete propylene oxide conversion, although the selectivity towards the desired product decreased. However, the nano–TiO$_2$ catalyst, after reaching steady state, was able to maintain its activity for at least 21 h, and no signs of deactivation were observed.

3.3. Catalytic mechanism

Fig. 7 illustrates the atomic network of nano–TiO$_2$, where coordinatively unsaturated Ti^{3+} Lewis atoms and oxygen vacancies can be found, associated in a single catalytic site. This acid–base pair, which only forms in oxide nanoparticles after some oxygen atoms of the lattice have left the network, is a fingerprint of vacant metal oxides, and thus could be responsible for the selective epoxide opening. If the reaction were to depend solely on the acidity of the catalyst, zirconium oxide should be more reactive, which is not the case. Moreover, the other vacant oxide tested, nano–CeO$_2$, was also active for the reaction (see Table 1) [32]. It has been reported that these vacancies are active
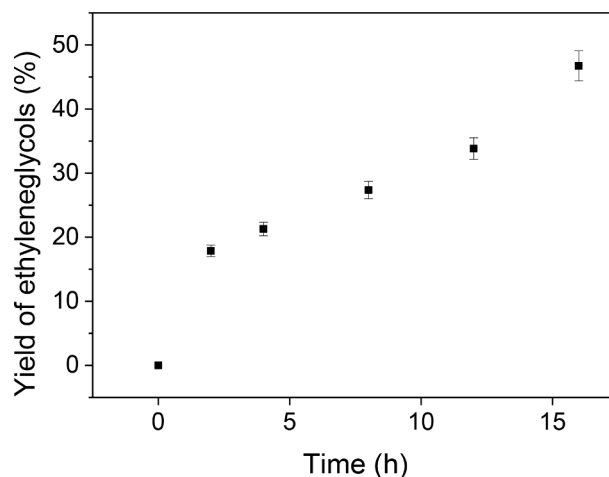

Fig. 2. Kinetics for the oligomerization of ethylene oxide **1a** in the presence of nano–TiO$_2$ (50 wt%) at 150 °C, followed by ^{1}H–NMR. Error bars represent 5% uncertainty.
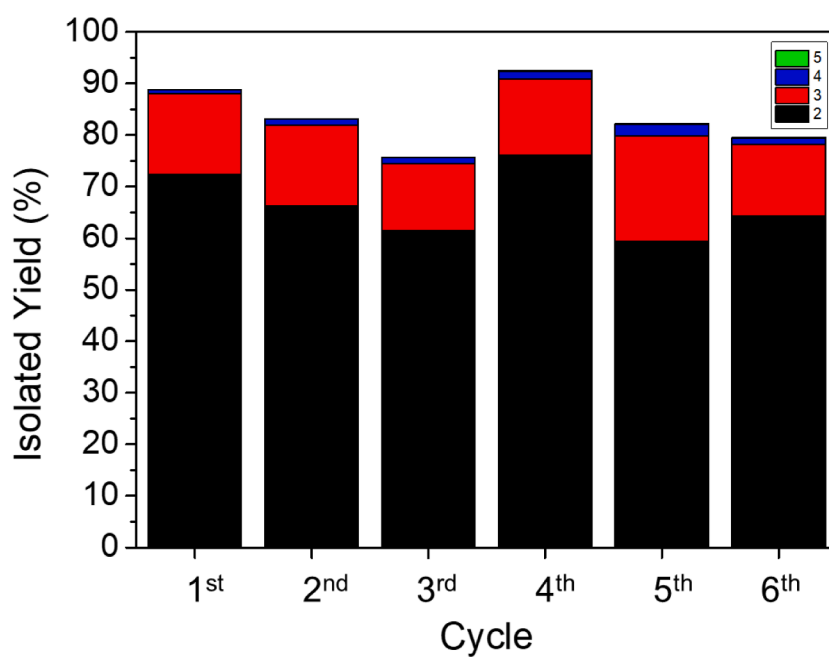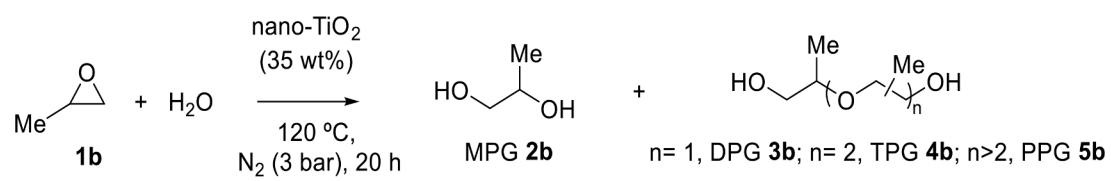
Fig. 3. Reusability of nano–TiO$_2$ for the hydration/oligomerization of propylene epoxide **1b** in the presence of water; $n > 5$ products are below 1%.
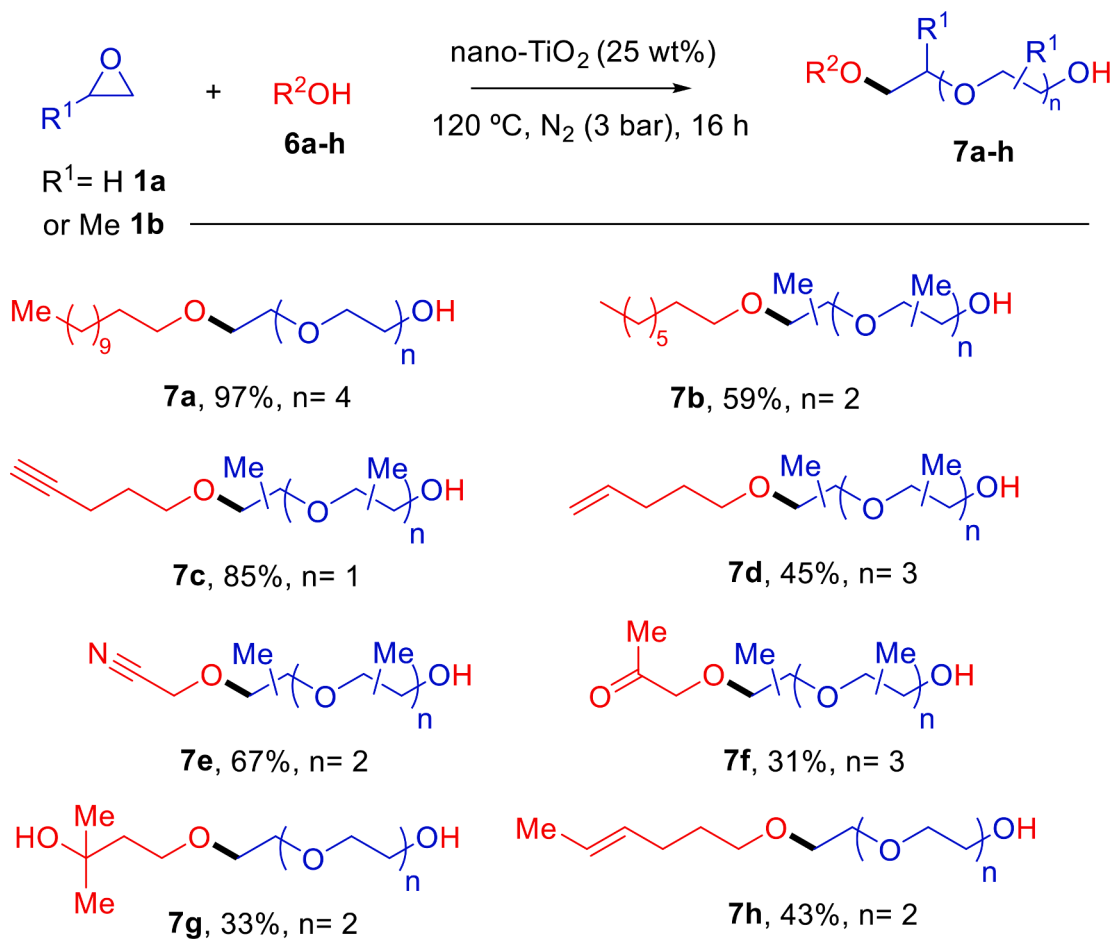
Fig. 4. Alkoxylated products with nano–TiO$_2$ catalyst at 120 °C during 16 h. The propoxylated products are a statistical mixture of methylated isomers.
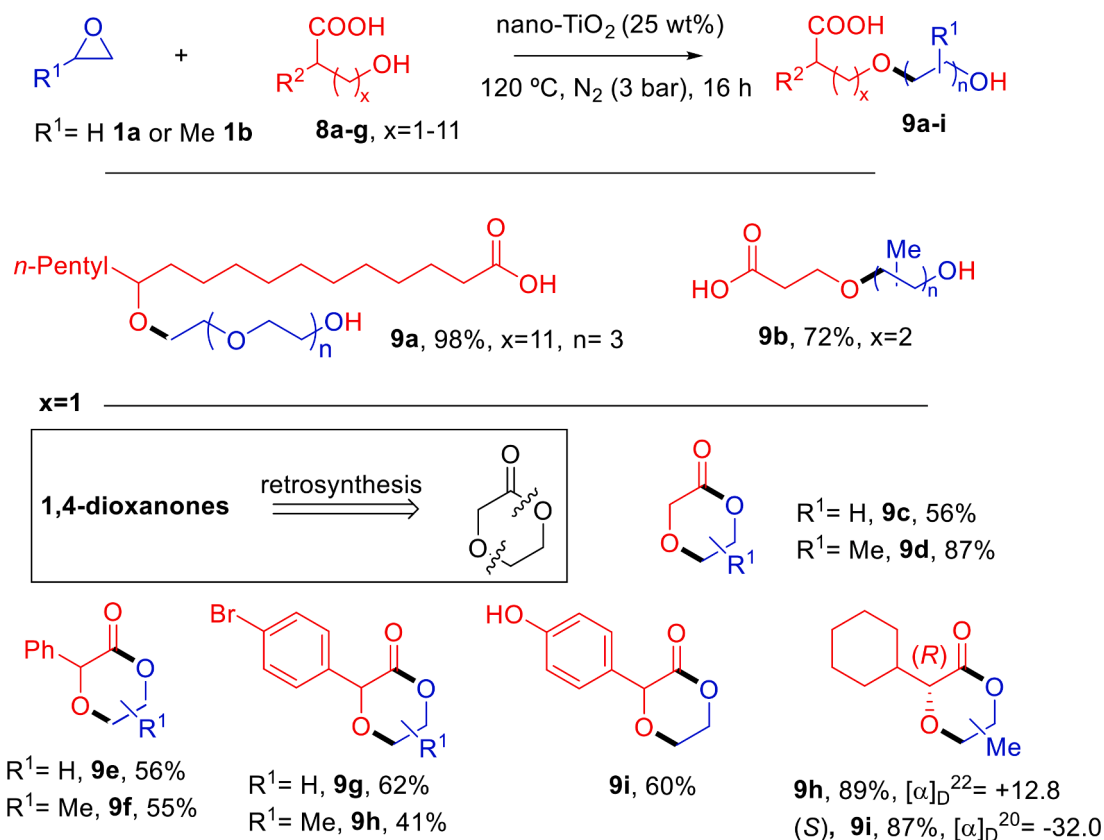
Fig. 5. Chemoselective alkoxylation of hydroxyacids and synthesis of 1,4–dioxenones with nano–TiO$_2$ catalyst at 120 °C during 16 h. The propoxylated products are a ~1:1 mixture of methylated isomers.

catalytic sites for different reactions and that the solid catalyst acts as a bifunctional acid/based catalyst [13]. In order to test this hypothesis, **1a** was reacted over a regular TiO$_2$ which contains chemical induced vacancies with ethanol, and the result showed that the vacant TiO$_2$ gave a 62% yield of glycols, much higher than regular TiO$_2$ (3%) and even nano–TiO$_2$ (42%), under the same reaction conditions. These results strongly supports the key role of the vacants in the catalytic process. To check if the crystallographic planes and the surface area also have a significant influence on the reaction rate, ceria nanocubes with a distinct surface area (41 vs 119 m$^2 \cdot$g^{-1}) but similar amount of vacancies than commercial nanoceria, and where these vacancies are exposed in the 100 instead than in the 111 crystallographic plane (Table S3), was prepared and used as a catalyst for the propoxylation reaction [29,30, 49]. High resolution–transmission electron microimages (HR–TEM) of the prepared catalytic nanocerias confirm the purity of the materials (Figure S11). The results show that no variation in the reaction rate occurs, thus discarding a key role of the exposed crystallographic plane and the surface area in the reaction outcome (Fig. 7) [50–52]. In order to further confirm the role of the vacancies, nanoceria doped with Al^{3+} was prepared and tested [51], and the reaction rate of epoxide opening was roughly 3 times higher than with regular nanoceria (Fig. 7). The nanoceria materials were calcined at >400 °C prior reaction in order to remove adsorbed carbonates [48].

Further tests in which nano-TiO$_2$ was treated with 10 mol% of either pyridine or di–*tert*–butylpyridine, were performed. Notice that while the former quenches the Lewis and Brönsted sites, the latter only quenches the Brönsted sites. The results (Figure S12) show that

di–*tert*–butylpyridine somewhat decreases the reaction rate, while pyridine is not informative because it catalyzes the reaction. These results suggest that acid sites in nano-TiO$_2$ may play a role during the catalysis, however, vacancies seem to be the main catalytic site for the epoxide opening [52,53]. This conclusion is in line with the catalytic results observed for the other nano–oxides (see Table above), since a combination of Lewis acidity and a high number of vacancies is what differentiates nano–TiO$_2$ from the rest of nano–oxides used as catalysts. Nano–ZrO$_2$ has less vacancies than nano TiO$_2$; nano MgO is basic, so the interaction of Mg atoms with the O atoms from the epoxide is not favored; and for CeO$_2$, it is well known that the bond Ti^{3+}-O (from the epoxide) is a stronger bond that Ce^{3+}-O, thus explaining the lower (but still) catalytic activity.

4. Conclusions

Nano–TiO$_2$ catalyzes the chemoselective hydration/alkoxylation of ethylene or propylene epoxide, to give glycols and alkoxylated products of similar chemical composition than commercial samples. Reactions occur without the need of corrosive, toxic and difficult to handle acids or bases, and avoids explosive by–processes. In contrast to strong bases, nanotitania preferentially activates alcohols over carboxylic acids, thus giving access to six–member ring gamma–oxo–esters (1,4–dioxanones). The vacancies of nano–TiO$_2$ seem to play a key role for the epoxide opening, behaving as a bifunctional site for epoxide and nucleophile activation. The nano–TiO$_2$ catalyzed process reported here not only provides access to commercial glycols and alkoxylated products in a
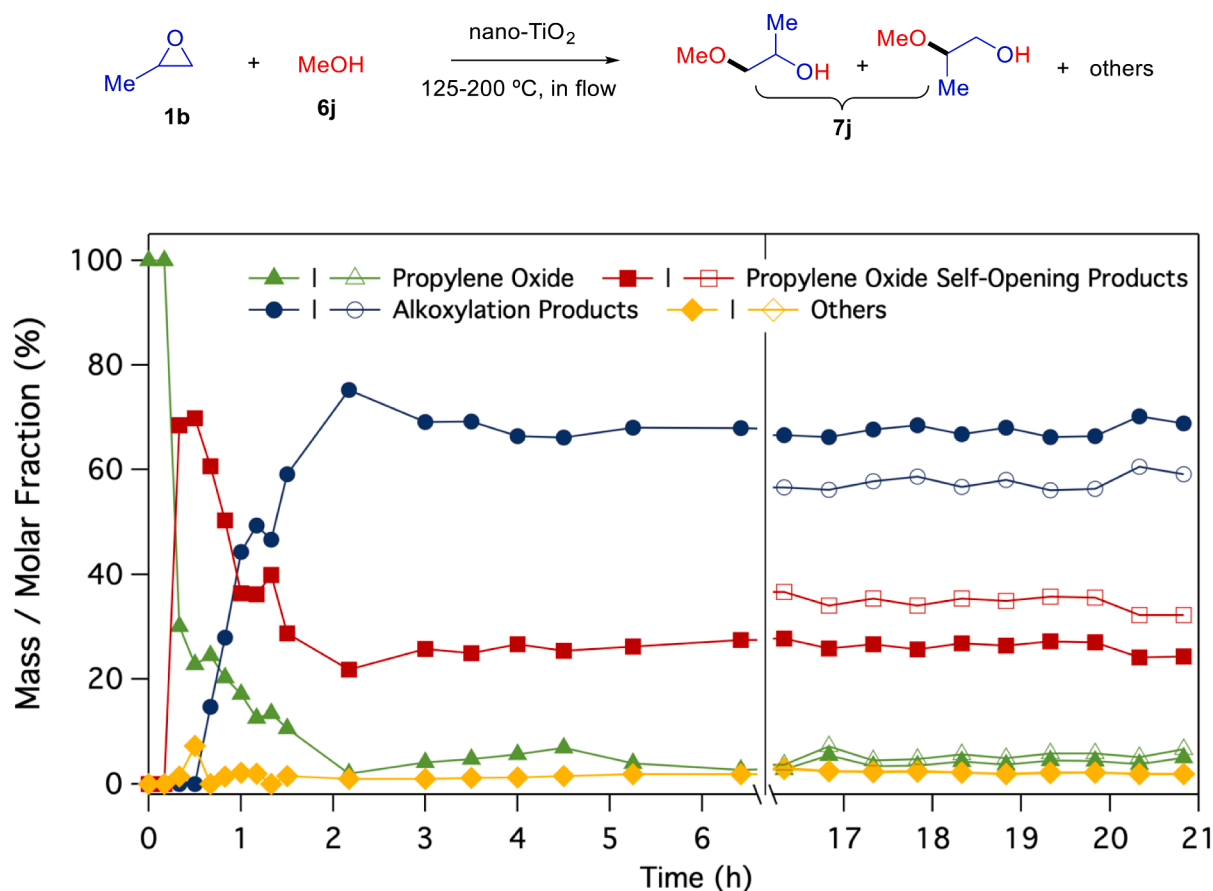
Fig. 6. Kinetic profiles of propylene oxide **1b**, alkoxylation products **7j** (1–methoxypropan–2–ol and 2–methoxypropan–1–ol), propylene oxide self–opening products **3b-5b**, and other products at the reactor outlet, during start–up and during the steady state. The filled markers represent the mass fraction; the hollow markers represent the molar fraction.
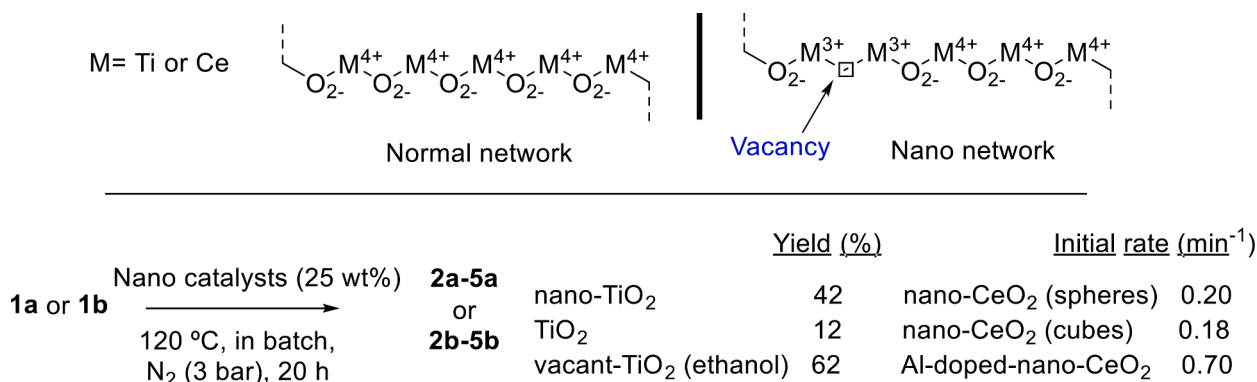

Fig. 7. Top: Schematic representation for the atomic network of regular and vacant metal oxides. Bottom: Yields (%) and initial rates (min^{-1}) of different titania and nanoceria materials during the epoxide opening of **1a** or **1b**, respectively. The nanoceria solids were calcined at >400 °C prior use.

simple and greener way, including in–flow processes, but also to new products of potential value.

Credit author statement

J.O.-M. performed and interpreted some catalytic experiments, including reuses and mechanistic studies. J.B.-S. performed and interpreted some of the reaction in flow. M.T.-S. performed and interpreted some of the reactions in batch and in flow, including mechanistic studies and characterization. A.M.-C. managed the industrial part, providing real samples of products and suggesting new lines of action. A.L.–P.

performed and interpreted some catalytic experiments, supervised the whole work and wrote the manuscript.

Declaration of Competing Interest

The authors have no competing interests to declare.

Acknowledgements

Supplementary materials

Supplementary material associated with this article can be found, in the online version, at doi:10.1016/j.mcat.2021.111927.

References

[1] S. Rebsdat, D. Mayer, Ethylene glycol, 13 (2000). https://doi.org/10.1002/14356007.a10_101.

[2] Z. Han, L. Rong, J. Wu, L. Zhang, Z. Wang, K. Ding, Catalytic hydrogenation of cyclic carbonates: a practical approach from CO2 and epoxides to methanol and diols, Angew. Chem., Int. Ed. 51 (2012) 13041–13045, https://doi.org/10.1002/anie.201207781.

[3] J. Hur, I. Moon, Novel ethylene oxide gas recovery system via hydrolysis in the dimethyl carbonate and monoethylene glycol production process, Ind. Eng. Chem. Res. 59 (2020) 3091–3096, https://doi.org/10.1021/acs.iecr.9b06344.

[4] G.-.W. Yang, Y.-Y. Zhang, R. Xie, G.-P. Wu, High-activity organocatalysts for polyether synthesis via intramolecular ammonium cation assisted SN2 ring-opening polymerization, Angew. Chem., Int. Ed. 59 (2020) 16910–16917, https://doi.org/10.1002/anie.202002815.

[5] L. Liu, A. Corma, Metal catalysts for heterogeneous catalysis: from single atoms to nanoclusters and nanoparticles, Chem. Rev. (Washington, DC, United States) 118 (2018) 4981–5079, https://doi.org/10.1021/acs.chemrev.7b00776.

[6] J.M. Asensio, D. Bouzouita, P.W.N.M. van Leeuwen, B. Chaudret, σ-H–H, σ-C–H, and σ-Si–H bond activation catalyzed by metal nanoparticles, Chem. Rev. 120 (2020) 1042–1084, https://doi.org/10.1021/acs.chemrev.9b00368.

[7] M. Viciano-Chumillas, M. Mon, J. Ferrando-Soria, A. Corma, A. Leyva-Pérez, D. Armentano, E. Pardo, Metal–organic frameworks as chemical nanoreactors: synthesis and stabilization of catalytically active metal species in confined spaces, Acc. Chem. Res. 53 (2020) 520–531, https://doi.org/10.1021/acs.accounts.9b00609.

[8] M. Rivero-Crespo, J. Oliver-Meseguer, K. Kapłońska, P. Kuśtrowski, E. Pardo, J. P. Cerón-Carrasco, A. Leyva-Pérez, Cyclic metal(oid) clusters control platinum-catalysed hydrosilylation reactions: from soluble to zeolite and MOF catalysts, Chem. Sci. 11 (2020) 8113–8124, https://doi.org/10.1039/D0SC02391D.

[9] J. Oliver-Meseguer, A. Domenech-Carbo, M. Boronat, A. Leyva-Perez, A. Corma, Partial reduction and selective transfer of hydrogen chloride on catalytic gold nanoparticles, Angew. Chem., Int. Ed. 56 (2017) 6435–6439, https://doi.org/10.1002/anie.201700282.

[10] M. Tejeda-Serrano, M. Mon, B. Ross, F. Gonell, J. Ferrando-Soria, A. Corma, A. Leyva-Pérez, D. Armentano, E. Pardo, Isolated Fe(III)-O sites catalyze the hydrogenation of acetylene in ethylene flows under front-end industrial conditions, J. Am. Chem. Soc. 140 (2018) 8827–8832, https://doi.org/10.1021/jacs.8b04669.

[11] D.E. Zavelev, G.M. Zhidomirov, R.A. Kozlovskii, Quantum chemical study of the mechanism of the catalytic oxyethylation of ethylene glycol on phosphorus-doped titanium dioxide: the role of the surface phosphoryl and hydroxyl groups of the catalyst, Kinet. Catal. 54 (2013) 157–167, https://doi.org/10.1134/S002315841302016X.

[12] B.M. Bhanage, S. Fujita, Y. Ikushima, M. Arai, Synthesis of dimethyl carbonate and glycols from carbon dioxide, epoxides, and methanol using heterogeneous basic metal oxide catalysts with high activity and selectivity, Appl. Catal. A Gen. 219 (2001) 259–266, https://doi.org/10.1016/S0926-860X(01)00698-6.

[13] A. Abad, P. Concepción, A. Corma, H. García, A collaborative effect between gold and a support induces the selective oxidation of alcohols, Angew. Chem., Int. Ed. 44 (2005) 4066–4069, https://doi.org/10.1002/anie.200500382.

[14] X. Zhang, W. Cui, W. Han, Y. Zhang, S. Liu, W. Mu, Y. Chang, R. Hu, Synthesis of propylene glycol methyl ether over amine modified porous silica, React, Kinet. Catal. Lett. 98 (2009) 349–353, https://doi.org/10.1007/s11144-009-0086-1.

[15] B. Li, S. Bai, X. Wang, M. Zhong, Q. Yang, C. Li, Hydration of Epoxides on [CoIII (salen)] Encapsulated in Silica-Based Nanoreactors, Angew. Chem., Int. Ed. 51 (2012) 11517–11521, https://doi.org/10.1002/anie.201203774.

[16] M. Zhong, Y. Zhao, Q. Yang, C. Li, Epoxides hydration on CoIII(salen)-OTs encapsulated in silica nanocages modified with prehydrolyzed TMOS, J. Catal. 338 (2016) 184–191, https://doi.org/10.1016/j.jcat.2016.03.006.

[17] Z. Liu, W. Zhao, F. Xiao, W. Wei, Y. Sun, One-pot synthesis of propylene glycol and dipropylene glycol over strong basic catalyst, Catal. Commun. 11 (2010) 675–678, https://doi.org/10.1016/j.catcom.2010.01.004.

[18] W. Dai, C. Wang, B. Tang, G. Wu, N. Guan, Z. Xie, M. Hunger, L. Li, Lewis acid catalysis confined in zeolite cages as a strategy for sustainable heterogeneous hydration of epoxides, ACS Catal. 6 (2016) 2955–2964, https://doi.org/10.1021/acscatal.5b02823.

[19] X. Liu, W. Mao, J. Jiang, X. Lu, M. Peng, H. Xu, L. Han, S. Che, P. Wu, Topotactic conversion of alkali-treated intergrown germanosilicate CIT-13 into single-crystalline ECNU-21 zeolite as shape-selective catalyst for ethylene oxide hydration, Chem. – A Eur. J. 25 (2019) 4520–4529, https://doi.org/10.1002/chem.201900173.

[20] M. Zhong, H. Li, J. Chen, L. Tao, C. Li, Q. Yang, Cooperative activation of cobalt–salen complexes for epoxide hydration promoted on flexible porous organic

frameworks, Chem. – A Eur. J. 23 (2017) 11504–11508, https://doi.org/10.1002/chem.201702810.

[21] Z.-.J. Yang, Y.-.F. Li, Q.-.B. Wu, N. Ren, Y.-.H. Zhang, Z.-.P. Liu, Y. Tang, Layered niobic acid with self-exfoliatable nanosheets and adjustable acidity for catalytic hydration of ethylene oxide, J. Catal. 280 (2011) 247–254, https://doi.org/10.1016/j.jcat.2011.03.026.

[22] E.M.G.A. Van Kruchten, R. Kunin, M.F. Lemanski, Acidic ion exchange resin as stabilizing additive in the hydrolysis of alkylene oxides, 2000.

[23] W. Derks, E.M.G.A. Van Kruchten, Catalytic process for producing an alkylene glycol from epoxides and water with reactor-output recycle, 2002.

[24] Y. Li, B. Yue, S. Yan, W. Yang, Z. Xie, Q. Chen, H. He, Preparation of ethylene glycol via catalytic hydration with highly efficient supported niobia catalyst, Catal. Lett. 95 (2004) 163–166, https://doi.org/10.1023/B:CATL.0000027290.25879.f2.

[25] E.M.G.A. Van Kruchten, Process for the preparation of alkylene glycols., 2009.

[26] W. Crudge, J.W. Van Hal, X. Zhang, Solid catalyst useful for converting alkylene oxide to alkylene glycol., 2009.

[27] H.C. Raths, W. Breuer, K. Friedrich, K. Herrmann, Use of hydrophobic hydrotalcites as alkoxylation catalysts., 1991.

[28] D. Kim, C. Huang, H. Lee, I. Han, S. Kang, S. Kwon, J. Lee, Y. Han, H. Kim, Hydrotalcite-type catalysts for narrow-range oxyethylation of 1-dodecanol using ethyleneoxide, Appl. Catal. A Gen. 249 (2003) 229–240, https://doi.org/10.1016/S0926-860X(03)00297-7.

[29] A. Leyva-Perez, D. Combita-Merchan, J.R. Cabrero-Antonino, S.I. Al-Resayes, A. Corma, Oxyhalogenation of activated arenes with nanocrystalline ceria, ACS Catal. 3 (2013) 250–258, https://doi.org/10.1021/cs300644s.

[30] A. Trovarelli, J. Llorca, Ceria catalysts at nanoscale: how do crystal shapes shape catalysis? ACS Catal. 7 (2017) 4716–4735, https://doi.org/10.1021/acscatal.7b01246.

[31] K. Rodney, P. Ann, Acetylenic diol ethylene oxide/propylene oxide adducts and their use in photoresist developers., 2002.

[32] F. Garnes-Portolés, M.Á. Rivero-Crespo, A. Leyva-Pérez, Nanoceria as a recyclable catalyst/support for the cyanosilylation of ketones and alcohol oxidation in cascade, J. Catal. 392 (2020) 21–28, https://doi.org/10.1016/j.jcat.2020.09.032.

[33] M. Tejeda-Serrano, M. Mon, B. Ross, F. Gonell, J. Ferrando-Soria, A. Corma, A. Leyva-Perez, D. Armentano, E. Pardo, Isolated Fe(III)-O sites catalyze the hydrogenation of acetylene in ethylene flows under front-end industrial conditions, J. Am. Chem. Soc. 140 (2018) 8827–8832, https://doi.org/10.1021/jacs.8b04669.

[34] K. O'Lenick, A.J. O'Lenick Jr., Acetylenic quaternary ammonium compounds useful as surfactants in cosmetic products., 2012.

[35] A.S. Karakoti, S. Singh, A. Kumar, M. Malinska, S.V.N.T. Kuchibhatla, K. Wozniak, W.T. Self, S. Seal, PEGylated nanoceria as radical scavenger with tunable redox chemistry, J. Am. Chem. Soc. 131 (2009) 14144–14145, https://doi.org/10.1021/ja9051087.

[36] A.S. Karakoti, S. Das, S. Thevuthasan, S. Seal, PEGylated Inorganic Nanoparticles, Angew. Chem., Int. Ed. 50 (2011) 1980–1994, https://doi.org/10.1002/anie.201002969.

[37] J. Cui, M. Björnmalm, Y. Ju, F. Caruso, Nanoengineering of Poly(ethylene glycol) particles for stealth and targeting, Langmuir 34 (2018) 10817–10827, https://doi.org/10.1021/acs.langmuir.8b02117.

[38] J. Herzberger, K. Niederer, H. Pohlit, J. Seiwert, M. Worm, F.R. Wurm, H. Frey, Polymerization of ethylene oxide, propylene oxide, and other alkylene oxides: synthesis, novel polymer architectures, and bioconjugation, Chem. Rev. 116 (2016) 2170–2243, https://doi.org/10.1021/acs.chemrev.5b00441.

[39] A.J. O'Lenick Jr., J.K. Parkinson, Group selectivity of ethoxylation of hydroxy acids, J. Soc. Cosmet. Chem. 44 (1993) 319–328.

[40] M.J. Climent, A. Corma, S.B.A. Hamid, S. Iborra, M. Mifsud, Chemicals from biomass derived products: synthesis of polyoxyethyleneglycol esters from fatty acid methyl esters with solid basic catalysts, Green Chem. 8 (2006) 524–532, https://doi.org/10.1039/B518082A.

[41] J.A. Faraldos, R.M. Coates, J.-L. Giner, Alternative synthesis of the colorado potato beetle pheromone, J. Org. Chem. 78 (2013) 10548–10554, https://doi.org/10.1021/jo4017056.

[42] S. Kirchmeyer, A. Mertens, M. Arvanaghi, G.A. Olah, Synthetic methods and reactions; 114. General procedure for the conversion of acetals and ketone acetals into 2-alkoxyalkanenitriles using cyanotrimethylsilane, Synthesis (Stuttg) (1983) 498–500, https://doi.org/10.1055/s-1983-30402.

[43] S. Musa, I. Shaposhnikov, S. Cohen, D. Gelman, Ligand–metal cooperation in PCP pincer complexes: rational design and catalytic activity in acceptorless dehydrogenation of alcohols, Angew. Chem., Int. Ed. 50 (2011) 3533–3537, https://doi.org/10.1002/anie.201007367.

[44] K. Chung, S.M. Banik, A.G. De Crisci, D.M. Pearson, T.R. Blake, J.V. Olsson, A. J. Ingram, R.N. Zare, R.M. Waymouth, Chemoselective Pd-catalyzed oxidation of polyols: synthetic scope and mechanistic studies, J. Am. Chem. Soc. 135 (2013) 7593–7602, https://doi.org/10.1021/ja4008694.

[45] X. Xie, S.S. Stahl, Efficient and selective cu/nitroxyl-catalyzed methods for aerobic oxidative lactonization of diols, J. Am. Chem. Soc. 137 (2015) 3767–3770, https://doi.org/10.1021/jacs.5b01036.

[46] Y. Ogiwara, K. Sato, N. Sakai, Palladium-catalyzed cyclization of alkynoic acids to form vinyl dioxanones bearing a quaternary allylic carbon, Org. Lett. 19 (2017) 5296–5299, https://doi.org/10.1021/acs.orglett.7b02572.

[47] W.C. Ho, K. Chung, A.J. Ingram, R.M. Waymouth, Pd-catalyzed aerobic oxidation reactions: strategies to increase catalyst lifetimes, J. Am. Chem. Soc. 140 (2018) 748–757, https://doi.org/10.1021/jacs.7b11372.

[48] P. Thapa, S. Hazoor, B. Chouhan, T.T. Vuong, F.W. Foss, Flavin nitroalkane oxidase mimics compatibility with NOx/TEMPO catalysis: aerobic oxidization of alcohols,

diols, and ethers, J. Org. Chem. 85 (2020) 9096–9105, https://doi.org/10.1021/acs.joc.0c01013.

[49] Y. Tang, R.I.L. Meador, C.T. Malinchak, E.E. Harrison, K.A. McCaskey, M. C. Hempel, T.W. Funk, Cyclopentadienone)iron-catalyzed transfer dehydrogenation of symmetrical and unsymmetrical diols to lactones, J. Org. Chem. 85 (2020) 1823–1834, https://doi.org/10.1021/acs.joc.9b01884.

[50] M. Nolan, S.C. Parker, G.W. Watson, The electronic structure of oxygen vacancy defects at the low index surfaces of ceria, Surf. Sci. 595 (2005) 223–232, https://doi.org/10.1016/j.susc.2005.08.015.

[51] M. Aresta, A. Dibenedetto, C. Pastore, C. Cuocci, B. Aresta, S. Cometa, E. De Giglio, Cerium(IV)oxide modification by inclusion of a hetero-atom: a strategy for producing efficient and robust nano-catalysts for methanol carboxylation, Catal. Today. 137 (2008) 125–131, https://doi.org/10.1016/j.cattod.2008.04.043.

[52] Y. Wang, F. Wang, Q. Song, Q. Xin, S. Xu, J. Xu, Heterogeneous ceria catalyst with water-tolerant lewis acidic sites for one-pot synthesis of 1,3-diols via prins condensation and hydrolysis reactions, J. Am. Chem. Soc. 135 (2013) 1506–1515, https://doi.org/10.1021/ja310498c.

[53] G. Wang, L. Wang, X. Fei, Y. Zhou, R.F. Sabirianov, W.N. Mei, C.L. Cheung, Probing the bifunctional catalytic activity of ceria nanorods towards the cyanosilylation reaction, Catal. Sci. Technol. 3 (2013) 2602–2609, https://doi.org/10.1039/C3CY00196B.